



Published in final edited form as:

*Angew Chem Int Ed Engl.* 2018 November 12; 57(46): 15040–15044. doi:10.1002/anie.201806483.

## Design of a multicompartment hydrogel that facilitates time-resolved delivery of combination therapy and synergized killing of glioblastoma

Poulami Majumder<sup>a</sup>, Ulrich Baxa<sup>b</sup>, Scott T. R. Walsh<sup>a</sup>, and Joel P. Schneider<sup>a</sup>

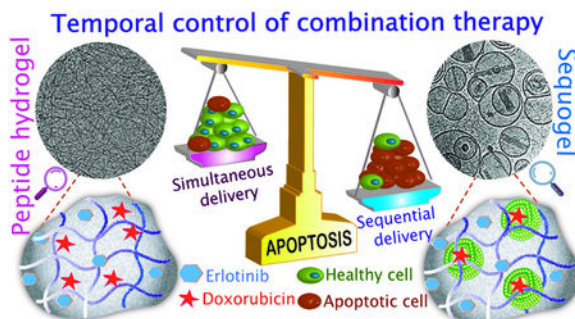
<sup>[a]</sup>Chemical Biology Laboratory, National Cancer Institute, 376 Boyles St Frederick MD 21702 USA

<sup>[b]</sup>National Cryo-Electron Microscopy facility, Frederick National Laboratory for Cancer Research, Frederick, MD 21702 USA

### Abstract

There is significant current interest in identifying new combination therapies that synergize to treat disease, and it is becoming increasingly clear that the temporal resolution of their administration greatly impacts efficacy. To facilitate effective delivery, we developed a multicompartment hydrogel material composed of spherical vesicles interlaced within a self-assembled peptide-based network of physically crosslinked fibrils that allows time-resolved independent co-delivery of small molecules. Herein, we demonstrate that this material architecture effectively delivers the EGFR kinase inhibitor erlotinib (ERL) and doxorubicin (DOX, DNA intercalator) in an ERL→DOX sequential manner to synergistically kill glioblastoma, the most aggressive form of brain cancer.

### Graphical Abstract



Divided We Stand: Time-resolved delivery of small molecule drugs achieved via an injectable multicompartment hydrogel material strongly synergizes their apoptotic activity in Glioblastoma

### Keywords

Peptide; Self-assembly; Hydrogel; Doxorubicin; Combination therapy

Supporting information for this article is given via a link at the end of the document.

Combination therapy administers multiple drugs having different mechanisms of action that together provide synergy.<sup>[1]</sup> Given the temporal resolution of biochemical pathways inherent in cancer progression, the differing PK/PD properties of individual agents, and the finding that oncogenic signaling can be rewired by drugs,<sup>[2]</sup> it is becoming clear that the time-specific administration of combination therapies can define their efficacy in cancer treatment. For example, previous studies showed that time-staggered administration of Paclitaxel followed by Flavopiridol provided significant apoptotic activity in breast and gastric cancer cells while simultaneous combination or the drugs applied in reverse order show modest effect.<sup>[3]</sup> It follows that developing singular materials that can deliver multiple drugs at differing rates should accompany current drug discovery efforts to identify promising new combination therapies.<sup>[4]</sup> Herein, we develop a syringe-deliverable, self-assembled multicompartiment hydrogel platform called ‘Sequogel’ that allows the time-staggered release of small molecule combination therapy and demonstrate its utility in affecting apoptosis in glioblastoma cells in a synergistic manner, Figure 1. We chose glioblastoma as a model system because it is one of the most aggressive forms of brain malignancy with current treatment protocols affording median survival rates of only 18 months. Further, it affords the opportunity to assess the synergistic activity of Erlotinib (ERL, an EGFR inhibitor). This drug failed to show significant responses in phase II clinical trials when administered as a monotherapy for glioblastoma.<sup>[5]</sup> However, it’s been found that treating phosphorylated EGFR-overexpressing cells, such as non-small cell lung cancer (NSCLC), with ERL rewires their apoptotic pathways and sensitizes them towards DNA damaging drugs, such as Doxorubicin (DOX).<sup>[2]</sup> ERL binds to the intracellular tyrosine kinase domain of both HER1/EGFR and EGFRVIII. Expression levels of HER1/EGFR in glioblastoma are similar (43–83%)<sup>[6]</sup> to those of NSCLCs and EGFRVIII is also expressed in both. Further, a delivery system that administers ERL and DOX in a time-staggered manner has recently been reported to be effective towards phosphorylated EGFR-overexpressing A549 lung and BT-20 breast cancer cells.<sup>[7]</sup> Thus, the benefit of sequentially administered ERL→DOX may prove efficacious for glioblastoma and we hypothesized that developing a soft material that could be delivered by syringe to tissue after tumor resection, and locally deliver these agents with independent temporal resolution may prove beneficial as an adjuvant.

Before developing a material for sequential delivery, we first tested the hypothesis that ERL and DOX could act synergistically to induce an apoptotic response in glioblastoma. LN229 human glioblastoma cells were incubated with increasing concentrations of ERL and DOX alone and in combination, administered simultaneously or sequentially. Annexin V coupled with propidium iodide staining was used to quantitate early and late apoptotic cells. ERL alone resulted in negligible response (Figure 2a,b, S1), which is in agreement with earlier report<sup>[2]</sup>. DOX alone induced a 21% apoptotic response when administered at 10 µM. This response increased in a non-additive fashion when ERL was co-administered simultaneously with DOX, and gratifyingly, increased significantly when ERL was added 24h before the DNA damaging small molecule. This observation was also evident in dose response where DOX alone provided an EC<sub>50</sub> of 17.6 µM, which decreased to 10.1 µM with an ERL→DOX administration, Figure 2b. The 24 h pre-treatment period was based on the earlier work of Yaffe et al <sup>[2]</sup>. The efficacy of time-dependent delivery was assessed in a dose-dependent

manner using both Bliss<sup>[8]</sup> and Chou-Talalay<sup>[9]</sup> methodology, Figure 2c and d. EGFR inhibition was synergistic with DOX in killing LN229 cells nearly across all concentrations tested (Table S1).

However, treating cells with either 10 or 15  $\mu\text{M}$  each of ERL and DOX in a sequential manner provided strong synergy with corresponding Excess Over Bliss (EOB) values of 30 and 22, respectively. In agreement, Chou-Talalay derived combination index (CI) values were 0.2 and 0.1 for the same concentrations (Table S1).

Having shown that synergy is possible, we developed a material called Sequogel comprised of a peptide-based fibrillar hydrogel that encapsulates ERL as well as DOX-loaded vesicles designed to deliver these agents in an ERL $\rightarrow$ DOX sequential manner, Figure 1. Gels with vesicular structures embedded within are a developing class of materials finding utility in delivery applications.<sup>[10]</sup> The hydrogel component of Sequogel is prepared using a self-assembling peptide (Figures 3a, S2).<sup>[11]</sup> Using triggerable self-assembling peptides allows facile encapsulation of precise concentration of drugs into the resulting gel matrix.<sup>[12]</sup> The peptide's sequence was designed to contain alternating hydrophobic and hydrophilic charged residues imbuing facial amphiphilicity which helps drive self-assembly. When the peptide is initially dissolved in low ionic strength buffer at pH 7.4, it exists as an unfolded monomer. Gelation can be triggered by adding additional buffer that contains 150 mM NaCl, which increases the solution's ionic strength and screens the peptide's charged lysine side-chains. This allows the unfolded monomer to self-assemble into a physically crosslinked fibrillar network rich in  $\beta$ -sheet secondary structure as shown by CD (Figure S3) and discussed later. When ERL and DOX-containing vesicles are present in the triggering buffer, they are directly encapsulated in the network during gel formation, Figure 3a. We envisioned that encapsulated ERL would be released in an early time-regime given its small molecular size and that the larger vesicles containing DOX would be released more slowly. As will be shown, the use of vesicles is necessary to retard the release rate of DOX from the gel network.

The gel's fibrillar network is positively charged due to the high content of protonated Lys residues, which can influence the behavior of its encapsulants via electrostatic interactions.<sup>[13]</sup> As such, the zeta potential of the vesicles proved critical to their behavior within, and release from the positively charged gel network. Neutral (PC/cholesterol), negatively charged (POPS/PC/cholesterol), and positively charged (DOTAP/PC/cholesterol, abbreviations are defined in Table S2) DOX loaded vesicles were prepared using a modified transmembrane pH gradient method<sup>[14]</sup> with an average encapsulation efficiency of ~95% (Table S3, Figure S4 shows original correlograms). All vesicles were stable at 4 °C for at least one month without significant changes in their hydrodynamic diameters or zeta potentials (Table S4, Figure S5). Figure 3b shows an experiment where differently charged DOX-loaded vesicles are encapsulated in a 1 wt% peptide gel. DOX release was then measured by UV-VIS as a function of time. DOX can be released either in the form of DOX-loaded vesicles or as free DOX, if the vesicles have been prematurely disrupted in the gel network. In order to measure the DOX contained within the released vesicles, vesicles were solubilized with the detergent Triton X-100 (1%, v/v) prior to the absorbance measurement. DLS size measurements were performed on released supernatant prior to detergent treatment

to determine if intact vesicles were being released as opposed to free DOX. The data in Figure 3b and the associated DLS data (Figure S6) show that DOX-loaded neutral and positively charged vesicles are released slowly from the gel network. Once released, separate experiments show that the vesicles can contain their encapsulated DOX for days, Figure S7. With respect to the negatively charged vesicles, DLS shows that they become compromised when encapsulated in the positively charged gel, resulting in the rapid release of free DOX. Thus, negatively charged vesicles are not compatible with the peptide gel network. Given their slightly slower release profile, the neutral vesicles were used for the final Sequogel formulation.

Figures 3c and S8a show cryo-transmission electron micrographs of DOX-loaded neutral vesicles encapsulated within the peptide gel network. Nano-assemblies, typical of entrapped DOX<sup>[14]</sup>, are clearly seen within the vesicles. The fibril network of the hydrogel is also observed, characterized by fibril widths (~2.5 nm) that are consistent with the peptide folding into a  $\beta$ -hairpin conformation, which is 3 nm in length, Figure 3a. Sequogel is prepared by directly encapsulating DOX-vesicles and ERL during hydrogel formation. We next assessed the influence of the encapsulates on peptide self-assembly and the rheological properties of the resultant gel. Cryo-TEM of peptide gel alone is shown in Figure S8b. Identical circular dichroism (CD) spectra of Sequogel containing ERL and DOX-vesicles versus peptide gel alone (Figure S3) with characteristic minima centered at 216 nm, indicates that peptide self-assembly leading to the formation of the  $\beta$ -sheet rich fibrillar hydrogel network is unaffected by the presence of the encapsulants. Figure 3d show time-sweep and shear-thin/recovery oscillatory rheology data. In the first stage of this experiment, the storage moduli ( $G'$ ) is monitored as a function of time after gelation is triggered for both peptide gel alone and Sequogel containing drugs. Next, the gels are shear-thinned and allowed to recover, simulating what they might experience during delivery via syringe injection. Both gels quickly recover after being thinned. Frequency and strain sweep data are shown in Figure S9. The nearly identical rheological behavior of the empty gel and Sequogel indicate that neither the vesicles nor ERL influence the mechanical properties of the gel network. Figures 3e and S10 show the release profile of ERL and DOX-loaded vesicles from Sequogel formulated with 15  $\mu$ g each of ERL and DOX. Again, released vesicles were solubilized with detergent Triton X-100 (1%, v/v) prior to analysis. Figure 3e shows release over 6 days, at which time only about 20% of total DOX had been released. The use of vesicles is important for the effective delivery of DOX. Free DOX (e.g. not encapsulated in vesicles) is released rather quickly from the gel network with about 80% being released in just 2 hours, Figure S10a. Figure S10b shows that ERL is indeed released from Sequogel in an early time regime as predicted with quantitative release occurring over 24 h. In contrast, DOX-vesicles are released from Sequogel much more slowly with less than 10% of the total DOX being released in the same 24 h period. The mesh size of Sequogel's fibrillar network can be estimated from rheology to be ~70 nm<sup>[13a]</sup>, slightly smaller than the average diameter of the encapsulated vesicles. Thus, it is likely that loosely associated vesicles near the solvent exposed surface of the gel and smaller diameter vesicles are initially released. Sterically restricted vesicles should be released much later. At any rate, the earlier apoptosis assays (Figure 2) suggest that the time differential in delivering the two agents afforded by Sequogel, with ERL being delivered in the first 24 h, should result in synergistic activity.

Though ERL released from Sequogel need only to bind to cell surface receptors to affect action, vesicles carrying DOX need to be internalized by cells for DOX to perform its action. Thus, we first determined the mechanism of vesicular uptake and the cellular distribution of DOX.

Doubly-labeled vesicles were used to visualize the internalization of intact vesicles into LN229 cells. Sequogels were prepared using vesicles loaded with FITC-dextran within the aqueous compartment and labeled with fluorescent rhodamine lissamine-PE within their lipid bilayer, Figure 4a. Cells cultured in the presence of Sequogel were imaged 4 h after being introduced to the gel. Live-cell imaging shows significant co-localization of green and red fluorescence within cells indicating that the small number of vesicles released at this time have been effectively internalized intact<sup>[15]</sup>. Next, the mechanism of vesicular uptake was investigated by flow cytometry. In the experiments outlined in Figure 4b, cells were incubated in the presence of Sequogel under endocytic-perturbing conditions. Clathrin-dependent pathways were blocked by pre-incubating cells with hyperosmolar sucrose<sup>[16]</sup>, resulting in a ~30% reduction in cellular uptake. General endocytic activity was further blocked by pre-incubating cells with sodium azide and 2-deoxy-D-glucose, which drains cellular ATP pools.<sup>[17]</sup>

This resulted in a ~45% reduction in vesicular uptake. Thus, endocytosis contributes significantly to vesicular uptake, which is in agreement with earlier work showing that neutral and anionic vesicles can enter cells through clathrin-mediated endocytic pathways<sup>[18]</sup>. The mechanism by which DOX is released from the vesicles is not known. However, separate experiments show that cells are able to accumulate increasing concentrations of DOX over time. Figure 4c shows that at 4 h, cells are accumulating detectable DOX, which increases at 16 h, consistent with a slow sustained release of vesicles from Sequogel. Internalized DOX eventually partitions to the nucleus, Figure 4d. It should be noted that the amount of vesicles released in the time-regime used for these internalization studies is small. The majority of DOX will be delivered in a later time-regime, after ERL has sensitized the cells. At any rate, the data indicate a mechanism where vesicles are taken up by cells, in part, by endocytic mechanisms.

The influence of sequentially delivered ERL and DOX on LN229 cells was studied in an in-vitro assay where Sequogel was introduced to a trans-well insert above a lawn of cells. Apoptosis was measured after 48 h, enough time for released ERL to sensitize the cells towards the slowly released DOX-containing vesicles. Figure 5a measures apoptotic response due to Sequogel compared to two control gels. The first control delivers ERL along with empty vesicles. The second control is void of ERL, and only delivers DOX-containing vesicles. The amount of drug in each formulation was also varied. Gels delivering only ERL had no effect as expected. The second control, delivering only DOX, resulted in 15–30% apoptotic response, increasing with DOX concentration. Importantly, Sequogel, delivering ERL→DOX vesicles, increased the apoptotic response to 40–59% over the same drug concentration range. This is impressive given the fact that Sequogel had only delivered ~15% of its initial DOX payload over the course of this experiment. Additional control experiments showed that empty gels, empty vesicles and empty Sequogels had no effect on their own, Figure S11a and b.

We also monitored the activation of caspase 3/7 through live-cell imaging as an alternative indicator of apoptosis, Figures 5b and S11c. Here, green fluorescence indicates increased caspase 3/7 activity. While control gel delivering ERL and empty vesicles and a second control gel delivering DOX vesicles results in a marginal increase in activity, Sequogel delivering ERL→DOX vesicles results in a significant increase (3-fold) in caspase 3/7 activity, mirroring the results outlined in Figure 5a.

The development of gels that can be injected into tissue during resection therapy will be useful adjuvants in treating glioblastoma where the blood-brain barrier has been surgically breached. Here, we demonstrate the utility of Sequogel, an injectable viscoelastic material capable of the time-resolved delivering of erlotinib and doxorubicin. The design premise of co-encapsulating free drug along with late-eluting vesicular carriers into a shear-thinning gel provides a versatile materials platform whose composition can be easily modified to deliver other combination therapeutics.

## Supplementary Material

Refer to Web version on PubMed Central for supplementary material.

## Acknowledgments

This research was supported by the Center for Cancer Research intramural research program of the National Cancer Institute, National Institutes of Health.

## References

- [1]. a)Sun W, Sanderson PE, Zheng W, *Drug Discov Today* 2016, 21, 1189–1195; [PubMed: 27240777] b)Bulusu KC, Guha R, Mason DJ, Lewis RP, Muratov E, Kalantar Motamedi Y, Cokol M, Bender A, *Drug Discov Today* 2016, 21, 225–238; [PubMed: 26360051] c)Zoli W, Ricotti L, Tesei A, Barzanti F, Amadori D, *Crit Rev Oncol Hematol* 2001, 37, 69–82; [PubMed: 11164721] d)Miles D, von Minckwitz G, Seidman AD, *Oncologist* 2002, 7 Suppl 6, 13–19. [PubMed: 12454315]
- [2]. Lee MJ, Ye AS, Gardino AK, Heijink AM, Sorger PK, MacBeath G, Yaffe MB, *Cell* 2012, 149, 780–794. [PubMed: 22579283]
- [3]. Motwani M, Delohery TM, Schwartz GK, *Clin Cancer Res* 1999, 5, 1876–1883. [PubMed: 10430095]
- [4]. Wang C, Wang J, Zhang X, Yu S, Wen D, Hu Q, Ye Y, Bomba H, Hu X, Liu Z, Dotti G, Gu Z, *Science Translational Medicine* 2018, 10.
- [5]. Vogelbaum MA, Peereboom D, Stevens G, Barnett G, Brewer C, *Journal of Clinical Oncology* 2004, 22, 121s–121s.
- [6]. Karpel-Massler G, Schmidt U, Unterberg A, Halatsch ME, *Molecular Cancer Research* 2009, 7, 1000–1012. [PubMed: 19584260]
- [7]. Morton SW, Lee MJ, Deng ZJ, Dreaden EC, Siouve E, Shopsowitz KE, Shah NJ, Yaffe MB, Hammond PT, *Science Signaling* 2014, 7.
- [8]. Bliss CI, *Ann Appl Biol* 1939, 26, 585–615.
- [9]. Chou TC, *Pharmacol Rev* 2006, 58, 621–681. [PubMed: 16968952]
- [10]. a)Boekhoven J, Koot M, Wezendonk TA, Eelkema R, van Esch JH, *J Am Chem Soc* 2012, 134, 12908–12911; [PubMed: 22823592] b)Wickremasinghe NC, Kumar VA, Hartgerink JD, *Biomacromolecules* 2014, 15, 3587–3595; [PubMed: 25308335] c)Collier JH, Hu BH, Ruberti JW, Zhang J, Shum P, Thompson DH, Messersmith PB, *J Am Chem Soc* 2001, 123, 9463–9464; [PubMed: 11562238] d)Arai T, Benny O, Joki T, Menon LG, Machluf M, Abe T, Carroll RS,

- Black PM, *Anticancer Research* 2010, 30, 1057–1064; [PubMed: 20530409] e) Lopez-Noriega A, Hastings CL, Ozbakir B, O'Donnell KE, O'Brien FJ, Storm G, Hennink WE, Duffy GP, Ruiz-Hernandez E, *Advanced Healthcare Materials* 2014, 3, 854–859. [PubMed: 24436226]
- [11]. a) Haines-Butterick L, Rajagopal K, Branco M, Salick D, Rughani R, Pilarz M, Lamm MS, Pochan DJ, Schneider JP, *Proceedings of the National Academy of Sciences of the United States of America* 2007, 104, 7791–7796; [PubMed: 17470802] b) Rajagopal K, Lamm MS, Haines-Butterick LA, Pochan DJ, Schneider JP, *Biomacromolecules* 2009, 10, 2619–2625. [PubMed: 19663418]
- [12]. a) Li Y, Wang F, Cui H, *Bioeng Transl Med* 2016, 1, 306–322; [PubMed: 28989975] b) Zhao F, Ma ML, Xu B, *Chem Soc Rev* 2009, 38, 883–891. [PubMed: 19421568]
- [13]. a) Branco MC, Pochan DJ, Wagner NJ, Schneider JP, *Biomaterials* 2009, 30, 1339–1347; [PubMed: 19100615] b) Branco MC, Pochan DJ, Wagner NJ, Schneider JP, *Biomaterials* 2010, 31, 9527–9534; [PubMed: 20952055] c) Medina SH, Li S, Howard OZ, Dunlap M, Trivett A, Schneider JP, Oppenheim JJ, *Biomaterials* 2015, 53, 545–553; [PubMed: 25890750] d) Nagy-Smith K, Yamada Y, Schneider JP, *Journal of Materials Chemistry B* 2016, 4, 1999–2007.
- [14]. Li XG, Hirsh DJ, Cabral-Lilly D, Zirkel A, Gruner SM, Janoff AS, Perkins WR, *Biochimica Et Biophysica Acta-Biomembranes* 1998, 1415, 23–40.
- [15]. Torchilin VP, Rammohan R, Weissig V, Levchenko TS, *Proceedings of the National Academy of Sciences of the United States of America* 2001, 98, 8786–8791. [PubMed: 11438707]
- [16]. Lakkaraju A, Rahman YE, Dubinsky JM, *Journal of Biological Chemistry* 2002, 277, 15085–15092. [PubMed: 11830589]
- [17]. Wrobel I, Collins D, *Biochimica Et Biophysica Acta-Biomembranes* 1995, 1235, 296–304.
- [18]. a) Poste G, Papahadjopoulos D, *Proceedings of the National Academy of Sciences of the United States of America* 1976, 73, 1603–1607; [PubMed: 818640] b) Straubinger RM, Hong K, Friend DS, Papahadjopoulos D, *Cell* 1983, 32, 1069–1079. [PubMed: 6404557]

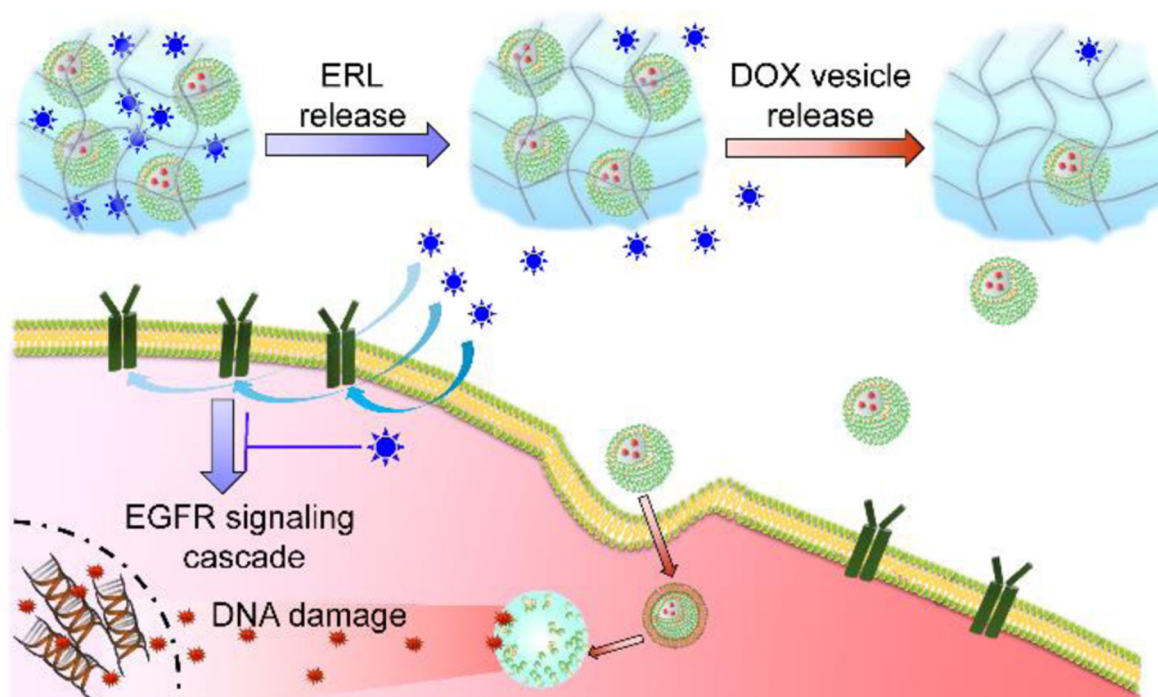


**Figure 1.** Schematic showing the time-staggered delivery of ERL and DOX-containing vesicles from Sequogel. ERL (blue stars) is released in an early time regime, inhibiting EGFR signaling, which sensitizes LN229 glioblastoma cells towards the action of DOX. DOX-loaded vesicles (green) are released slowly in a later time regime. Endocytosed vesicles release DOX (red stars), which enters the nucleus and intercalates within DNA inducing apoptosis.



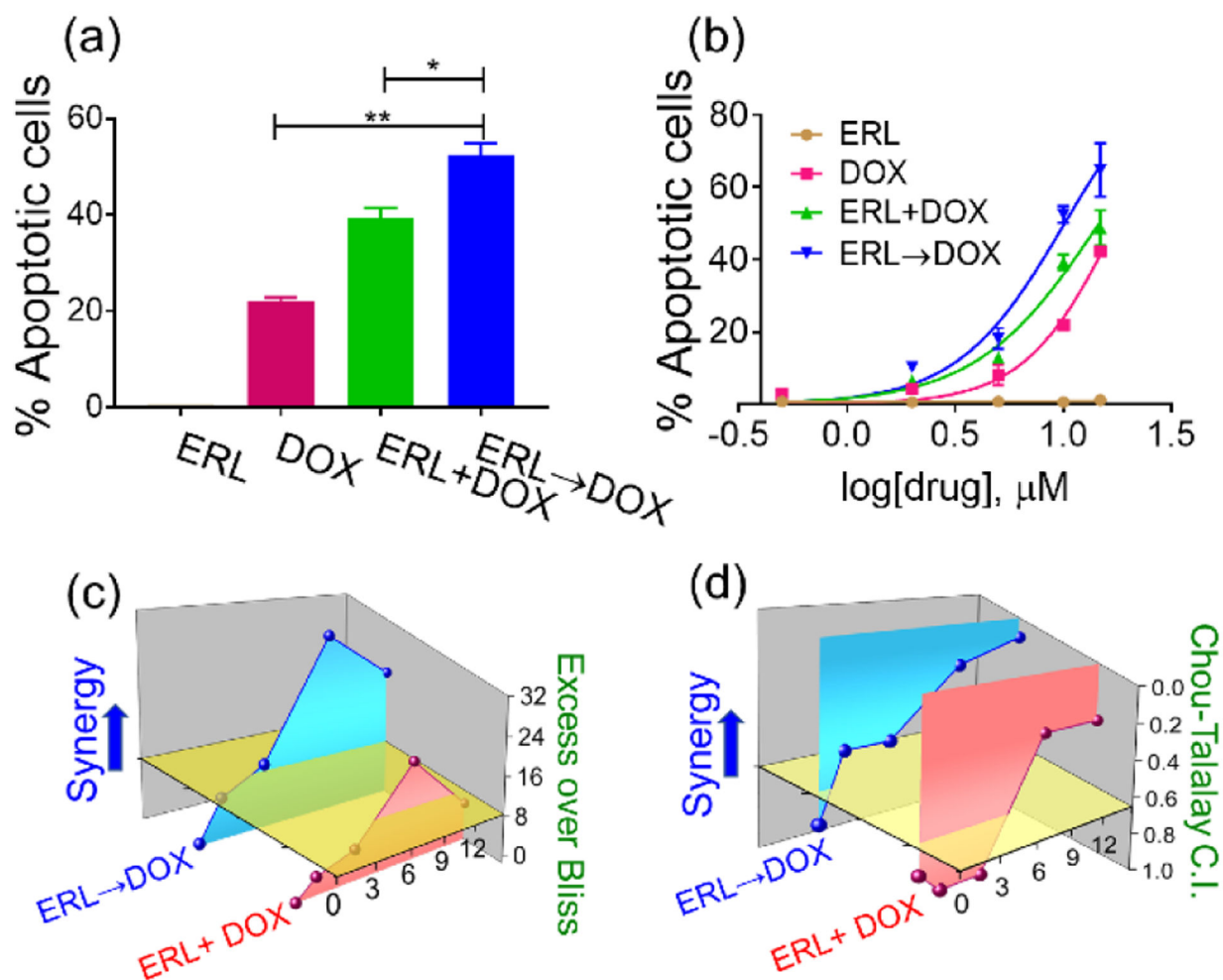


**Figure 2.**

(a) Apoptosis of LN229 cells treated with 10  $\mu\text{M}$  ERL alone for 42 h, 10  $\mu\text{M}$  DOX alone for 18 h, simultaneous delivery of ERL + DOX for 18 h, or sequential administration of ERL->DOX where cells are treated with ERL for 24 h followed by DOX for an additional 18 h. \*  $p < 0.05$ , \*\*  $p < 0.01$ . (b) Dose response curves for the different treatment schedules. Dose-dependent (c) Excess Over Bliss (EOB) and (d) Combination Index (CI) values for both simultaneous and sequential delivery of ERL and DOX.



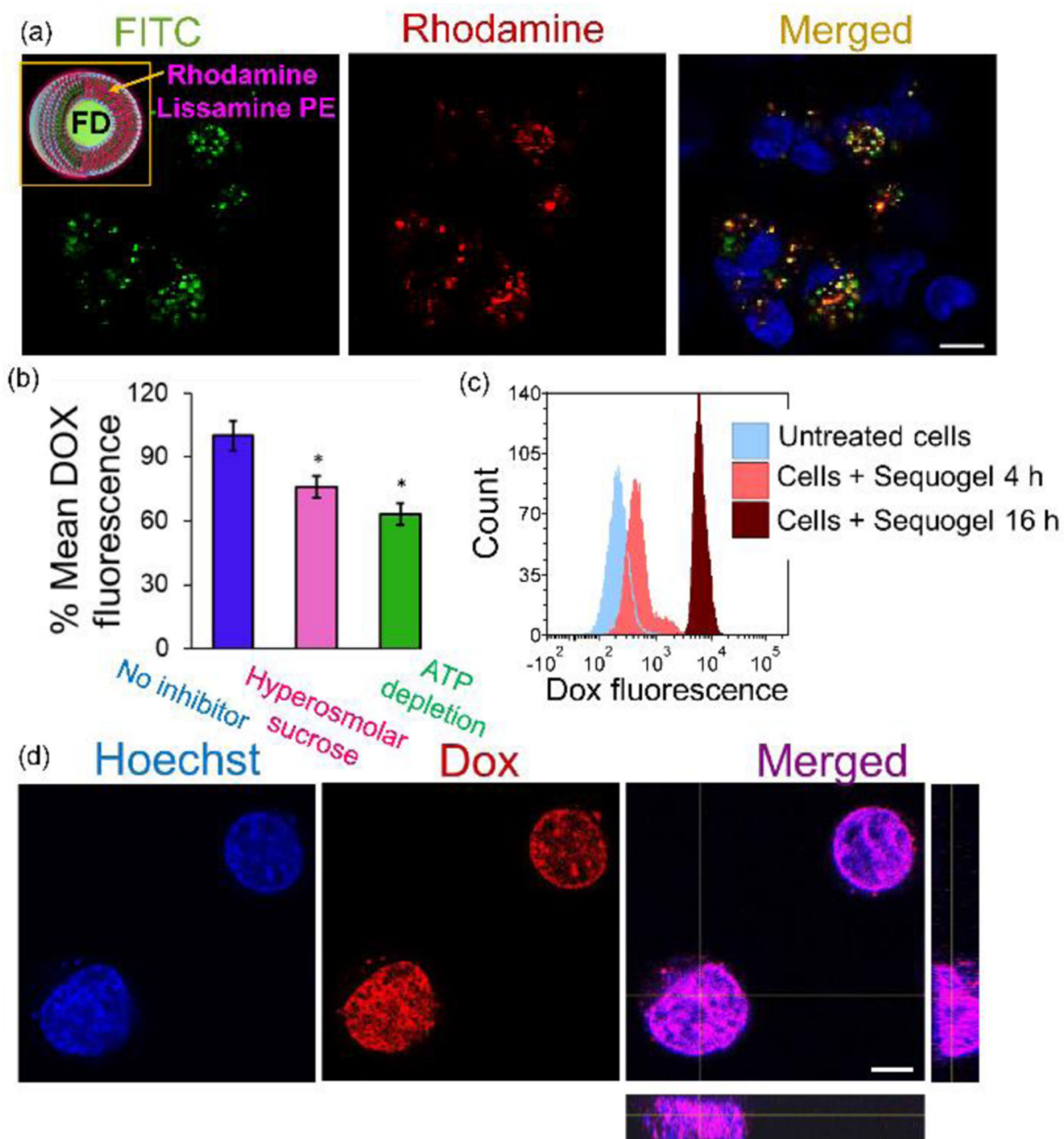


**Figure 4.**

(a) LN229 cellular uptake and localization of labeled vesicles released from Sequogel. Labeled vesicles encapsulate FITC-dextran (FD, green) within their aqueous core and contain Rhodamine lissamine-PE (red) in their lipid bilayer. (b) Mechanism of cellular uptake of DOX-loaded vesicles released from Sequogel. Cells were incubated with Sequogel for 1 h with and without endocytic inhibitors. Mean fluorescence intensities of DOX under each inhibition condition were compared to those in absence of inhibitor to determine statistical significance, indicated by \* for  $p < 0.05$ . (c) Representative histograms from flow cytometric detection of DOX internalization 4 h and 16 h post-incubation with Sequogel. (d)

Live-cell imaging of LN229 cells after addition of Sequogel containing DOX vesicles and ERL at 16 h post-incubation.

Author Manuscript

Author Manuscript

Author Manuscript

Author Manuscript

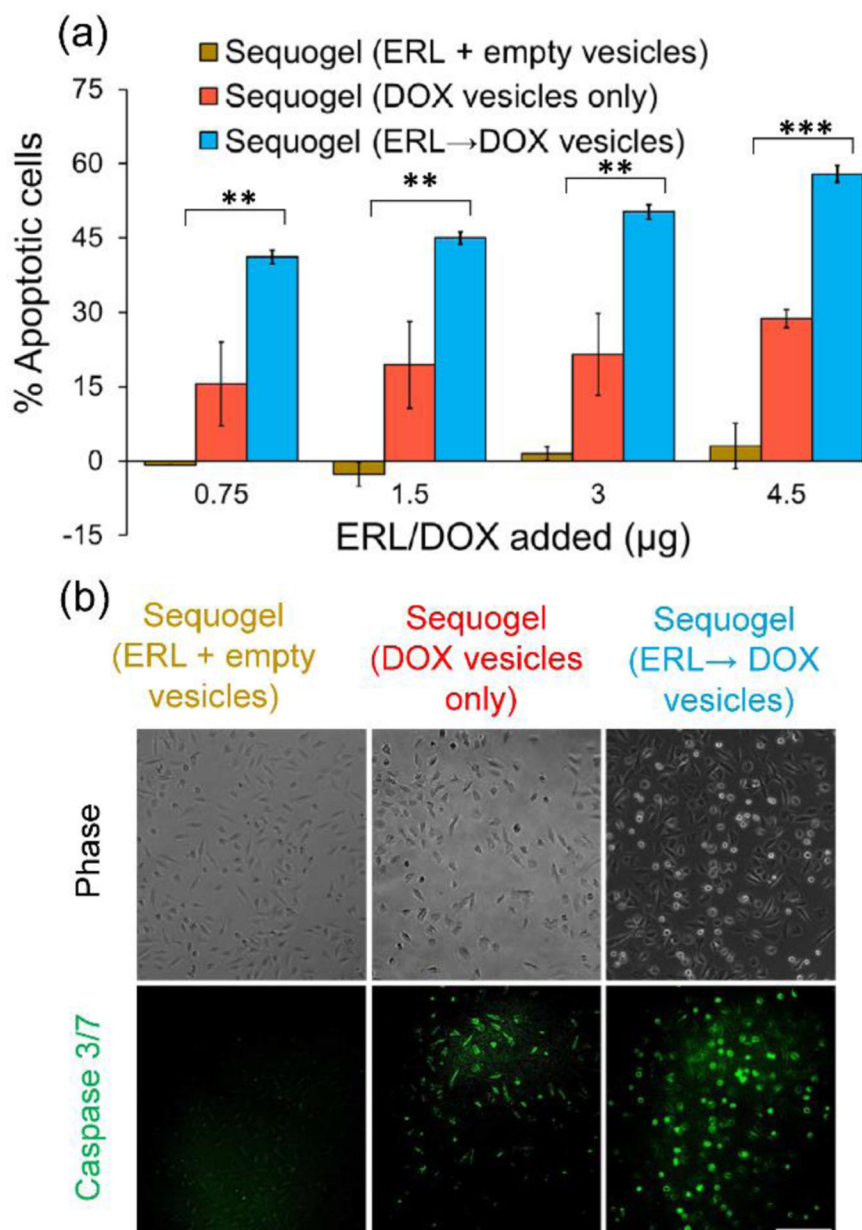


**Figure 5.**

(a) Flow cytometry quantifying the percentage of apoptotic LN229 cells resulting from treatment with different Sequogel formulations 48 h post-incubation. Statistical significance among different groups is indicated by \*\* for  $p < 0.01$  and \*\*\* for  $p < 0.001$ . (b) Determination of Caspase 3/7 activation in LN229 cells treated with different Sequogel formulations for 48 h. Green fluorescence indicates activated caspase 3/7. Scale bar 200 µm.